Combustion heat release analysis of ethanol or n-butanol diesel fuel blends in heavy-duty DI diesel engine

ARTICLE *in* FUEL · MAY 2011

Impact Factor: 3.52 · DOI: 10.1016/j.fuel.2010.12.003

4 AUTHORS, INCLUDING:

Dimitrios C. Rakopoulos
National Technical University of Athens
43 PUBLICATIONS **2,251** CITATIONS
SEE PROFILE

Dimitris C. Kyritsis
Khalifa University of Science Technology &…
55 PUBLICATIONS **911** CITATIONS
SEE PROFILE

Fuel 90 (2011) 1855–1867

Contents lists available at ScienceDirect

Fuel

journal homepage: www.elsevier.com/locate/fuel

Combustion heat release analysis of ethanol or *n*-butanol diesel fuel blends in heavy-duty DI diesel engine

D.C. Rakopoulos [a], C.D. Rakopoulos [a,*], R.G. Papagiannakis [b], D.C. Kyritsis [c]

[a] *Internal Combustion Engines Laboratory, Department of Thermal Engineering, School of Mechanical Engineering, National Technical University of Athens, Zografou Campus, 9 Heroon Polytechniou St., 15780 Athens, Greece*
[b] *Thermodynamic & Propulsion Systems Section, Aeronautical Sciences Department, Hellenic Air Force Academy, Dekelia Air Force Base, 1010 Dekelia, Attiki, Greece*
[c] *University of Illinois at Urbana Champaign, Department of Mechanical Science and Engineering, 1206 West Green Street, Urbana, IL 61801, USA*

ARTICLE INFO

Article history:
Received 30 August 2010
Received in revised form 17 October 2010
Accepted 6 December 2010
Available online 17 December 2010

Keywords:
Heavy-duty DI diesel
Combustion
Ethanol
n-Butanol
Emissions

ABSTRACT

An experimental study is conducted to evaluate the effects of using blends of diesel fuel with either ethanol in proportions of 5% and 10% or *n*-butanol in 8% and 16% (by vol.), on the combustion behavior of a fully-instrumented, six-cylinder, turbocharged and after-cooled, heavy duty, direct injection (DI), 'Mercedes-Benz' engine installed at the authors' laboratory. Combustion chamber and fuel injection pressure diagrams are obtained at two speeds and three loads using a developed, high-speed, data acquisition and processing system. A heat release analysis of the experimentally obtained cylinder pressure diagrams is developed and used. Plots of histories in the combustion chamber of the heat release rate and temperatures reveal some interesting features, which shed light into the combustion mechanism when using these promising bio-fuels that can be derived from biomass (bio-ethanol and bio-butanol). The key results are that with the use of these bio-fuels blends, fuel injection pressure diagrams are very slightly displaced (delayed), ignition delay is increased, maximum cylinder pressures are slightly reduced and cylinder temperatures are reduced during the first part of combustion. These results, combined with the differing physical and chemical properties of the ethanol and *n*-butanol against those for the diesel fuel, which constitutes the baseline fuel, aid the correct interpretation of the observed engine behavior performance- and emissions-wise.

1. Introduction

Apart from engine-related techniques to meet stringent imposed emissions regulations [1–4], engine researchers have focused their interest on the domain of fuel-related techniques, such as for example alternative gaseous fuels of renewable nature or oxygenated fuels that are able to reduce particulate emissions [5–9].

Considerable attention has been paid in the development of alternative fuel sources in various countries, with emphasis on bio-fuels that possess the added advantage of being renewable [10–13]. Bio-fuels made from agricultural products (oxygenated by nature) reduce the world's dependence on oil imports, support local agricultural industries and enhance farming incomes and, moreover, offer benefits in terms of usually reduced exhaust emissions. Among those, vegetable oils, their derived bio-diesels (methyl or ethyl esters) and bio-alcohols are considered as very promising fuels. Bio-fuel production is a rapidly growing industry in many parts of the world. Bio-ethanol is the primary alternative at present to gasoline for spark-ignition engines, and vegetable oils, their derived bio-diesels and bio-ethanol mixed with diesel fuel for diesel engines. However, other bio-fuels such as bio-butanol [14–17], biomass-derived hydrocarbon fuels and hydrogen are being researched at present, being regarded as the next generation bio-fuels [10].

The main disadvantages of vegetable oils, as diesel fuels, are associated with the highly increased viscosity, 10–20 times greater than the normal diesel fuel. To solve this problem, the following usual methods are adopted: blending in small blend ratios with diesel fuel, micro-emulsification with methanol or ethanol, cracking, and conversion into bio-diesels mainly through the transesterification process [18,19]. The advantages of bio-diesels as diesel fuel are the minimal sulfur and aromatic content, and higher flash point, lubricity, cetane number, biodegradability and non-toxicity. On the other hand, their disadvantages include the higher viscosity and pour point, the lower calorific value and volatility, lower oxidation stability and hygroscopic tendency. For all the above reasons, it is generally accepted that blends of diesel fuel, with up to 20% bio-diesels and vegetable oils, can be used in existing diesel engines without modifications. Experimental works on the use of

* Corresponding author. Tel.: +30 210 7723529; fax: +30 210 7723531.
E-mail addresses: cdrakops@central.ntua.gr (C.D. Rakopoulos), kyritsis@uiuc.edu (D.C. Kyritsis).

0016-2361/$ - see front matter © 2010 Elsevier Ltd. All rights reserved.
doi:10.1016/j.fuel.2010.12.003

vegetable oils or bio-diesels in blends with diesel fuel for diesel engines have been reported for example in Refs. [13,20–27].

Greece is now attempting to conform with the 2003/30 EC directive and to produce bio-diesel using oils available from the current agricultural activities, as well as from cultivations of new oil plants with improved oil production and land utilization [28]. A recent work by the authors [13] studied and compared an extended variety of vegetable oils and bio-diesels of various origins tested in blends with the normal diesel fuel. A companion paper extended the above investigation for the cottonseed oil and its methyl ester for up to 100/0 blend ratios, i.e. in neat forms [23].

The acute pollution problem of the major Athens area in Greece has urged the Athens Urban Transport Organization to show a vivid interest for the use of bio-fuels from Greek origin feedstock, such as vegetable oils, bio-diesels, bio-ethanol and bio-butanol in its bus fleet. Related works on those bus engines have been reported by this research group, for the purpose of investigating their performance and exhaust emissions behavior [16,22,29]. Further, the present researchers have published similar works for a HSDI (high speed direct injection) diesel engine of the automotive type using the same bio-fuels [13,17,23,30–34].

There seems to be an obvious scarcity of theoretical models scrutinizing the formation mechanisms of combustion-generated emissions when using liquid bio-fuels, unlike the advanced models existing for the study of diesel engines using conventional diesel fuel [1,35]. Recently, a detailed multi-zone combustion modeling with ethanol/diesel blends has been reported [36] by this research group, along the lines of a similar paper [37] applied for a HSDI Ricardo/Cussons 'Hydra', standard, experimental diesel engine when using vegetable oils or their derived bio-diesels, which has in turn been expanded on a similar multi-zone one dealing only with the related physical processes [38].

As a 'bridging' agent to correctly interpret the previous ethanol/diesel blends results and assist the multi-zone combustion modeling, a heat release analysis for the relevant combustion mechanism, combined with the widely differing physical and chemical ethanol properties against those for the diesel fuel, were used by the authors in [31] for the above HSDI diesel engine running with ethanol/diesel fuel blends at the same operating conditions. Also, a companion work has appeared [32], evaluating its combustion characteristics using experimental-stochastic techniques [39] and its propensity for combustion cyclic irregularity due to the low cetane number of ethanol [40]. Recently, a paper has appeared by the authors [33], for the same HSDI engine and conditions, dealing with the combustion heat release analysis of neat vegetable (cottonseed) oil or its neat bio-diesel. Further, a paper is reported by the authors [34], investigating the combustion of *n*-butanol/diesel fuel blends and its cyclic variability in the same HSDI diesel engine and conditions, using experimental heat release and stochastic analysis techniques.

1.1. Ethanol in diesel engines

Because of its high octane number, ethanol is a good spark-ignition engine fuel [2], but it is true that alcohols, mainly ethanol and to a much lesser extent methanol, have been considered as alternative fuels for diesel engines too [12,41–45]. Methanol can be produced from coal or petrol based fuels with low cost production, but it has a restrictive solubility in the diesel fuel. On the other hand, ethanol is a biomass-based renewable fuel, which can be produced by alcoholic fermentation of sugar from vegetable materials, such as corn, sugar cane, sugar beets, barley, sweet sorghum, cassava, molasses and the like, and agricultural residues, such as straw, feedstock and waste woods by using already improved and demonstrated technologies. Therefore, it has the advantage over methanol of higher miscibility with the diesel fuel and of being of renewable nature (bio-ethanol).

Two recent works have been reported by the group headed by the second author [30,31] concerning the use of ethanol blends, up to a blending ratio of 15/85 (by vol.), in a naturally aspirated, four-stroke, HSDI, Ricardo/Cussons 'Hydra' diesel engine of the automotive (car) type.

While anhydrous ethanol is soluble in gasoline, additives must be used in order to ensure solubility of anhydrous ethanol (that is highly hygroscopic) in diesel fuel under a wide range of conditions. Especially at lower temperatures the miscibility is limited. Moreover, adding ethanol to diesel fuel can reduce lubricity and create potential wear problems in sensitive fuel pump designs. Ethanol possesses also lower viscosity and calorific value, with the latter imposing minor changes on the fuel delivery system for achieving the engine maximum power [46–48]. By all estimates, ethanol has a very low cetane number that reduces the cetane level of the diesel–ethanol blend, requiring normally the use of cetane enhancing additives that improve ignition delay and mitigate cyclic irregularity [49–51]. Ethanol has much lower flash point than the diesel fuel and higher vapor formation potential in confined spaces, thus requiring extra precautions in its handling [12].

Various techniques have been developed to make diesel engine technology compatible with the properties of ethanol-based fuels. Broadly speaking, they can be divided into the following three classes: (a) Ethanol fumigation to the intake air charge, by using carburetion or manifold injection, which is associated with limits to the amount of ethanol that can be used in this manner, due to the incipience of engine knock at high loads, and prevention of flame quenching and misfire at low loads [44,52–54], (b) Dual injection system that is not considered very practical, as requiring an extra high-pressure injection system and a related major design change of the cylinder head [44], and (c) Blends (emulsions) of ethanol and diesel fuel by using an emulsifier to mix the two fuels for preventing their separation, requiring no technical modifications on the engine side [44,55–58].

It is mentioned that stable emulsions usually refer to both solutions of anhydrous ethanol in diesel fuel (transparent) and micro-emulsions of ethanol in diesel fuel (translucent). Anhydrous ethanol (200 proof) does not require an emulsifying agent or so called 'surfactant' to form a transparent solution in diesel fuel, but these solutions can tolerate only up to 0.5% water. Then, in the practical cases of using lower proof ethanol (say 190 proof or lower), an emulsifying agent is required to form the opaque macro-emulsion; this, however, could be separated into the two phases if allowed to stagnate for a long period [44]. Blends with up to 15% (by vol.) ethanol in diesel fuel are considered relatively safe from the engine durability point of view.

Inside the framework of the attempt for ramping up bio-fuels production, the Greek Ministry of Agriculture is asking the European Commission for permission to convert two of Greece's five existing sugar (beet) plants, owned by the 'Hellenic Sugar Industry SA', into bio-ethanol production facilities. If approved, Greece would dedicate some 50% of its current European Union quota for sugar beet to meet the demand created by these two plants, thus supporting the 'Hellenic Sugar Industry SA' and also the sugar beet producers by giving them the option to continue cultivation of the crop. This company is the sole sugar producer in Greece and is functioning inside the framework of the common agricultural policy of the European Union for the production and the disposal of sugar.

1.2. Butanol in diesel engines

A very strong alcohol competitor for use as fuel in diesel engines is *n*-butanol, which, nonetheless, has been hardly experimented

with on diesel engines. Butanol is of particular interest as a renewable bio-fuel as it is less hydrophilic and it possesses higher heating value, higher cetane number, lower vapor pressure, and higher miscibility than ethanol, making butanol preferable to ethanol for blending with conventional diesel fuel. Therefore, the problems associated with ethanol as a diesel fuel, mentioned in the previous subsection, are solved to a considerable extent when using *n*-butanol, which has properties much closer to diesel fuel than ethanol [10,59,60].

Like ethanol, butanol is a biomass-based renewable fuel that can be produced by alcoholic fermentation of the biomass feedstocks referred to above (bio-butanol). It is very coincidental that new and innovative processes for managing and utilizing the crude glycerol co-product from the bio-diesel production processes have been developed [61], which convert, for example, by anaerobic fermentation [62] the crude glycerol to significant yields of the value added products of mainly butanol, and 1,3-propanediol (PDO) and ethanol. This is really fortunate, since the increasing demand of bio-diesel production causes serious problems with the disposal of the by-produced crude glycerol (amounting to 10% by weight of the total) by the bio-diesel producers, given that its conversion to pure glycerol is no longer financially feasible due to the falling prices of the vast quantities available then for its market uses.

Butanol ($CH_3(CH_2)_3OH$) has a 4-carbon structure and is a more complex alcohol (higher-chain) than ethanol as the carbon atoms can either form a straight chain or a branched structure, thus resulting in different properties. Then, it exists as different isomers depending on the location of the hydroxyl group (–OH) and carbon chain structure, with butanol production from biomass tending to yield mainly straight chain molecules. 1-Butanol, also better known as *n*-butanol (normal butanol), has a straight-chain structure with the hydroxyl group (–OH) at the terminal carbon [10]. This is the isomer used in the present study.

The open literature concerning the use of butanol/diesel fuel blends in diesel engines and its effects on their performance and exhaust emissions is nearly absent. In Ref. [63], a two-cylinder, naturally aspirated, indirect injection (IDI) diesel engine of older design was tested at one speed with two butanol/diesel fuel blends. In reference [14], a drive cycle analysis of *n*-butanol/diesel blends in a light-duty turbo-diesel vehicle was reported. In Ref. [15], the influence of the diesel fuel *n*-butanol content on the performance and emissions of a heavy-duty DI diesel engine was investigated, with multi-injection fuel capability at fixed engine speed and load, and exhaust gas recirculation rates adjusted to keep NO_x emissions constant. Two more works by another research group [64,65] deal with the performance and exhaust emission characteristics of diesel engine fueled with vegetable oils blended with oxygenated organic compounds, including ethanol and *n*-butanol. Also, in Ref. [66] a very small quantity of *n*-butanol was used only for the purpose of improving the solubility of the ethanol/diesel fuel blends used.

Filling this gap, the present research group published a paper with the results of a similar investigation on a standard experimental, Ricardo/Cussons 'Hydra', high speed, naturally aspirated, direct injection (DI) diesel engine of automotive type [17], reporting the beneficial effects of using various blends of *n*-butanol with normal diesel fuel, with 8%, 16% and 24% (by vol.) *n*-butanol, on the performance and exhaust emissions at various loads. Consideration of theoretical aspects of diesel engine combustion and of the widely differing physical and chemical properties of the ethanol against those for the diesel fuel were used to aid, in a rather qualitative way, the interpretation of the observed engine behavior with these blends.

Furthermore, the present research group published recently the results of such an experimental investigation in a fully-instrumented, six-cylinder, water-cooled, turbocharged and after-cooled, heavy duty (HD), direct injection (DI), 'Mercedes-Benz', mini-bus diesel engine located at the authors' laboratory, by evaluating the effects of using various blends of *n*-butanol with normal diesel fuel, with 8% and 16% (by vol.) *n*-butanol, on the performance and exhaust emissions at two engine speeds and three loads with encouraging results [16]. Also, a work appeared recently, investigating the emissions during acceleration of that diesel engine operating with bio-diesel or *n*-butanol diesel fuel blends [67].

1.3. Ethanol and n-butanol in present work

As mentioned above, preliminary performance and emissions results have been reported with either the use of ethanol/diesel fuel [29] or *n*-butanol/diesel fuel blends [16] for the six-cylinder, water-cooled, turbocharged and after-cooled, heavy duty (HD), direct injection (DI), 'Mercedes-Benz' diesel engine concerning the present work. The interpretation of the experimental measurements was based there solely on the differences of properties between the fuels tested.

In this work, for the same blends and operating conditions, a heat release analysis is performed for studying the relevant combustion mechanism, along the lines of similarly conducted works for a HSDI, 'Ricardo/Cussons, 'Hydra', single-cylinder, standard experimental engine operated with either ethanol/diesel fuel [31], or *n*-butanol/diesel fuel blends [34], or neat vegetable cottonseed oil or its derived neat (methyl ester) bio-diesel [33]. As known, concerning the study of the combustion process in diesel engines, a very important means to analyze combustion characteristics is the calculation and analysis of heat release rates according to actual measurements of pressures in the (main) chamber (and the pre-chamber, if any) [31,68–70]. A companion diagram of the fuel injection pressure assists towards this side too.

The experimental cylinder pressure (indicator) diagrams, from the present DI engine, are directly processed in connection with the pertinent application of the energy and state equations. Attention is paid to the experimental work related to the specially developed, high-speed data (signal) acquisition and processing system. The results of the analysis for the rates of heat release and other related parameters in the combustion chamber reveal some very interesting features of the combustion mechanism, associated with the use of these promising bio-fuels. The combustion results, combined with the differing physical and chemical properties of the ethanol and *n*-butanol against those for the diesel fuel, which constitutes the 'baseline' fuel, aid the correct interpretation of the observed engine behavior performance- and emissions-wise when running with these bio-fuel blends.

2. Description of the engine and test facility

Facilities to monitor and control engine variables were installed on a test-bed, 'Mercedes-Benz' OM 366 LA, six-cylinder, heavy duty, direct injection, four-stroke, water-cooled, diesel engine located at the second author's laboratory. The engine is turbocharged with a 'Garrett' TBP 418-1 turbocharger and an air-to-air aftercooler after the turbocharger compressor. It is widely used to power medium trucks and mini-buses, as in the present case of the Athens Urban Transport Organization (AUTO) sub-fleet. It is coupled in the laboratory to a 'Schenck' U1-40 hydraulic brake (dynamometer), which is a variable fill brake with the loading accomplished via the brake lever that controls the amount of water swirling inside the machine. The basic data for the engine and injection system are shown in Table 1. The static injection timing of these engines is reduced up to a value of 5° CA (degrees Crank Angle) before TDC (Top Dead Center) at high loads, for the purpose of reducing nitrogen oxides emissions to meet the Euro II emission

Table 1
Engine and injection system basic data.

Engine model and type	'Mercedes-Benz', OM 366 LA, six-cylinder, in-line, four-stroke, compression ignition, direct injection, water-cooled, turbocharged, after-cooled
Speed range	800–2600 rpm
Engine total displacement	5958 cm^3
Bore/stroke	97.5 mm/133 mm
Connecting rod length	230 mm
Compression ratio	18:1
Firing order	1-5-3-6-2-4
Maximum power	177 kW @ 2600 rpm
Maximum torque	840 Nm @ 1250–1500 rpm
Inlet valve opening	15° crank angle before top dead center
Inlet valve closure	25° crank angle after bottom dead center
Exhaust valve opening	68° crank angle before bottom dead center
Exhaust valve closure	12° crank angle after top dead center
Fuel pump	'Bosch' PE-S series, in-line, six-cylinder, with 'Bosch' variable-speed mechanical governor
Injector body and nozzle	'Bosch', with five injector nozzle holes and opening pressure of 250 bar
Turbocharger	'Garrett' TBP 418–1
After-cooler	Air-to-air

standards [1]. Fig. 1 provides a full schematic arrangement of the engine test bed, instrumentation and data logging system.

A custom made tank and flow metering system is used for fuel consumption measurements of the various blend samples as follows. A glass burette of known volume was used with the time measured for its complete evacuation of the fuel sample feeding the engine. A system of pipes and valves was constructed in order to have a quick drain of a fuel sample, including the return-fuel from the pump and injector, and the refill of metering system with the new fuel sample.

The exhaust gas analysis system consists of a group of analyzers for measuring soot (smoke), nitrogen oxides (NO_x), carbon monoxide (CO) and total unburned hydrocarbons (HC). The smoke level in the exhaust gas was measured with a 'Bosch' RTT-100 opacimeter, the readings of which are provided as smoke opacity in % Hartridge units, or equivalent smoke (soot) density (milligrams of soot per cubic meter of exhaust gases). The nitrogen oxides concentration in ppm (parts per million, by vol.) in the exhaust was measured with a 'Signal' Series-4000 chemiluminescent analyzer (CLA) and was fitted with a thermostatically controlled heated line. The CO concentration (in ppm) in the exhaust was measured with a 'Signal' Series-7200 non-dispersive infrared analyzer (NDIR) equipped with a 'Signal' Series-2505 M Cooler. The total unburned hydrocarbons concentration (in ppm) in the exhaust was measured with a 'Ratfisch-Instruments' Series RS55 flame-ionization detector (FID) and was also fitted with a thermostatically controlled heated line.

Standard instruments measuring speed, pressures, temperatures, etc., were used. For measuring the pressure in one of the cylinders, a 'Kistler' miniature piezoelectric transducer is used, mounted to the cylinder head and connected to a 'Kistler' charge amplifier. Also, a 'Kistler' piezoelectric transducer connected to a 'Kistler' charge amplifier is used, fitted on the injector side of the pipe linking the injection pump and injector, to provide the fuel pressure signal. The signal from a 'Tektronix' TDC magnetic pick-up marker is used for time reference and speed measurements.

The output signals from the magnetic pick-up and the two piezoelectric transducers signals, while they are continuously monitored on a dual beam 'Tektronix 7313' storage oscilloscope, are connected to the input of a 'Keithley' DAS-1801ST A/D board installed on an IBM compatible Pentium III PC. This high-speed data acquisition board utilizes also dual-channel Direct Memory Access (DMA) operation. Control of this system is achieved by using an in-house developed computer code based on the 'TestPoint' control software.

3. Properties of fuels tested, mixing and selection of blending ratios

The conventional diesel fuel was supplied by the Aspropyrgos Refineries of the 'Hellenic Petroleum SA' and represents the typical,

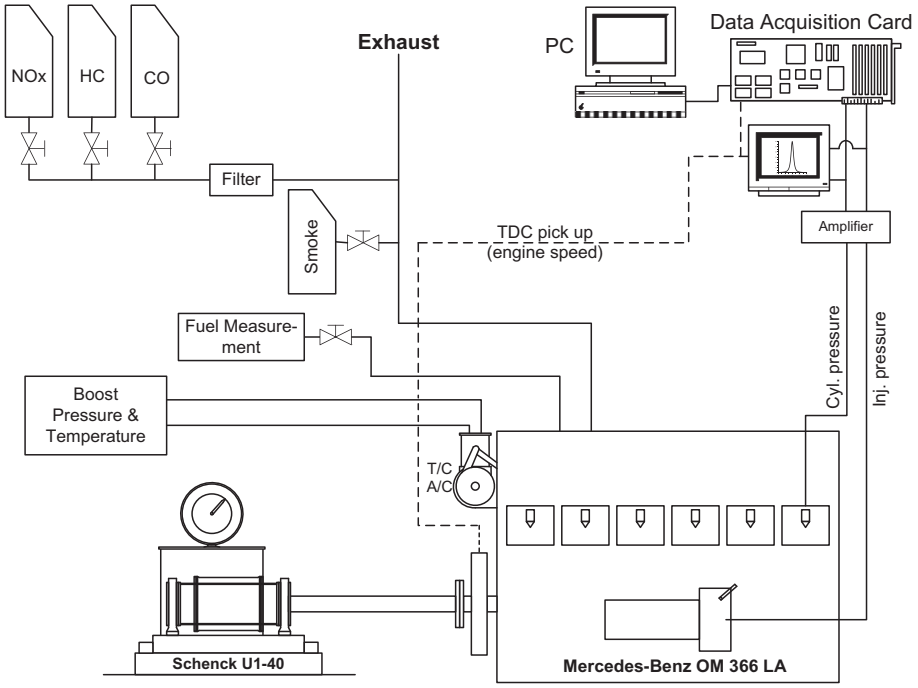

Fig. 1. Schematic arrangement of the engine test bed, instrumentation and data logging system.

Greek road (automotive), low sulfur (0.035% by weight) diesel fuel (gas oil); it formed the baseline fuel of the present study.

The ethanol (CH_3CH_2OH) of 99% purity is blended with the normal diesel fuel at blending ratios of 5/95 and 10/90 (by vol.). For the present experiments, no cetane improving additives (ignition improvers) were used. An emulsifying agent by 'Betz GE', a division of General Electric Inc., was used in proportions of 1.5% by volume, to satisfy mixture homogeneity and prevent phase separation. The emulsifier replaced a corresponding part of the diesel fuel. Thus, the 10/90 blend ratio corresponds to 88.5% diesel fuel, 1.5% emulsifier and 10% ethanol (by vol.), and similarly for the other blend. The mixing protocol consisted of first blending the emulsifier into the ethanol and then blending this mixture into the diesel fuel.

The isomer of butanol (C_4H_9OH) *n*-butanol (otherwise called 1-butanol), having a straight-chain structure and the hydroxyl group (–OH) at the terminal carbon, was used in the present study. It was of 99.9% purity (analytical grade). It was blended with the normal diesel fuel at blending ratios of 8/92 and 16/84 (by vol.). Preliminary evaluation tests on the solubility of *n*-butanol in the diesel fuel with blending ratios up to 40/60 proved, actually, that the mixing was excellent with no phase separation at all for a period of several days. Then, no emulsifying agent was necessary.

The properties of the diesel fuel, the ethanol and the *n*-butanol are summarized in Table 2. Only the density and lower calorific values were used in the computations, with all the other cited properties referred to here for comparative purposes, in order to explain qualitatively the relative performance and emissions behavior of the different fuel blends.

The selection of low blending percentages for ethanol or *n*-butanol is dictated by the necessity to avoid any cyclic combustion irregularity phenomena, which make their presence in diesel engines when very low cetane number fuels (cf. values in Table 2) are used [32,40].

On the other hand, the rationale for selecting the specific blending ratios with diesel fuel, i.e. of 5/95 and 10/90 for ethanol as against 8/92 and 16/84 for *n*-butanol, is that 5% ethanol or 8% *n*-butanol in the blend gives almost the same percentage of fuel-bound oxygen in the blend (cf. their oxygen contents in Table 2), and the same holds true for the 10% ethanol or 16% *n*-butanol in the blend. In this way, the comparison of the corresponding blends for ethanol and *n*-butanol is effected on the premise of an almost equal parameter, which is known to affect strongly the combustion behavior, via the 'local' fuel–air ratio in the various 'zones' and, consequently, the temperatures and emissions formation. Note that the air aspirated by the engine is constant for the same load and speed conditions. Of course, other parameters such as mainly viscosity, cetane number and calorific value are not then, in general, equal.

Table 2
Properties of diesel fuel, ethanol and *n*-butanol.

Fuel properties	Diesel fuel	Ethanol C_2H_5OH	*n*-Butanol C_4H_9OH
Density at 20 °C (kg/m^3)	837	788	810
Cetane number	50	~8	~25
Lower calorific value (MJ/kg)	43	26.8	33.1
Kinematic viscosity at 40 °C (mm^2/s)	2.6	1.2	3.6[a]
Boiling point	180–360	78	118
Latent heat of evaporation (kJ/kg)	250	840	585
Oxygen (% weight)	0	34.8	21.6
Bulk modulus of elasticity (bar)	16,000	13,200	15,000
Stoichiometric air–fuel ratio	15.0	9.0	11.2
Molecular weight	170	46	74

[a] Measured at 20 °C.

4. Parameters tested and experimental procedure

The series of tests are conducted using each of the above mentioned blends of either ethanol or *n*-butanol, with the engine working at speeds of 1200 and 1500 rpm, and at three loads of 20%, 40% and 60% of the full load, corresponding to brake mean effective pressures (b.m.e.p.) of 3.56, 7.04 and 10.52 bar, respectively. Owing to the differences among the calorific values and oxygen contents of the fuels tested, the comparison is effected at the same engine brake mean effective pressure (load) and not at the same injected fuel mass or air-to-fuel ratio.

In each test, volumetric fuel consumption rate, exhaust smokiness and exhaust regulated gas emissions such as nitrogen oxides, carbon monoxide and total unburned hydrocarbons are measured. From the first measurement, the specific fuel consumption and thermal efficiency are computed using the fuel sample density and lower calorific value. Table 3 shows the accuracy of the measurements and the uncertainty of the computed results of the various parameters tested.

At the same time, during each test, combustion chamber (indicator) and fuel injection pressure diagrams were obtained using the specially developed data acquisition system described above. The heat release analysis of these experimentally obtained cylinder pressure diagrams is outlined in the next section. The pressures are measured with accuracy better than within ±1% of full-scale output (fso, 200 bar), and the accuracy of the analog input readings of the data acquisition system is within ±0.01%.

The experimental work started with a preliminary investigation of the engine fueled with neat diesel fuel in order to determine the engine operating characteristics and exhaust emission levels, constituting the 'baseline' that is compared with the corresponding cases when using the ethanol/diesel or *n*-butanol/diesel fuel blends. The same procedure was repeated for each fuel blend by keeping the same operating conditions. For every fuel change, the fuel lines were cleaned and the engine was left to operate for about 30 min to stabilize at its new desired condition.

5. Theory of the experimental heat release analysis

5.1. Preliminary treatment of the measured pressure diagrams

The method of processing the experimental cylinder pressure diagrams and their analysis for heat release has been reported in detail in previous publication by the authors, as for example in Ref. [31] for a DI (direct injection) diesel engine and in Ref. [70] for the more complicated case of an IDI (indirect injection) diesel engine. Therefore, only a brief outline will be provided here.

A recording is made of the cylinder (indicator) pressure data for ten cycles in a contiguous file, with a sampling rate corresponding to 0.5° CA. A signal from a magnetic pick-up, which is simultaneously

Table 3
Accuracy of measurements and uncertainty of computed results.

Measurements	Accuracy
Smoke opacity	±0.1%
NO_x	±5 ppm
Time	±0.5%
Speed	±2 rpm
Torque	±0.5 N m
Computed results	Uncertainty (%)
Fuel volumetric rate	±1
Power	±1
Specific fuel consumption	±1.5
Efficiency	±1.5

recorded, indicates the position of the TDC in each cycle. Further, by considering the TDC position of any two consecutive cycles and knowing the sampling rate of the measurements (e.g., in the present case, at 0.5° CA with a nominal speed of 1200 or 1500 rpm), the calculation of the accurate engine speed in each cycle from the first to the last one is easily achieved. Pressure data points required in-between the experimentally acquired ones are obtained by interpolation. Then, the 'mean' of the cylinder (indicator) and the fuel pressure diagrams are obtained, while a 'light smoothing' for the pressure signals is applied that is based on performing a six-data points weighted smoothing. This seems to offer a reasonable compromise between no loss of valuable signal information and of relatively smooth values for the first derivative of pressure with respect to crank angle φ.

It is recognized that the application of heat release rate (HRR) analysis requires special care. As also mentioned in a recent paper [71], ad hoc methods and experience-based algorithms are mostly used, and there is not a consensus in the scientific community about the optimal way to proceed. Then, every research group as the present one, with vast experience since a long time ago on HHR analysis, judges and chooses the right way for its application. Of course, one of the main problems with the method of piezoelectric transducer/charge amplifier system (used by almost all investigators) is the 'noise' in the computation of the pressure derivative signal. In Ref. [72], a new promising method is proposed, in which a cylinder pressure analog variation signal is obtained directly from the measurement system, thus avoiding its computation.

5.2. Energy conservation and state equations

The measured pressure data to be processed for the heat release analysis concern the closed part of the thermodynamic cycle. A spatial uniformity of pressure p, temperature T and composition in the combustion chamber (single-zone model), at each instant of time t (with corresponding cylinder volume V) or during a crank angle step $d\varphi$, is assumed.

By combining the first law of thermodynamics and the perfect gas equation of state in differential form for the cylinder gas content, the net heat release Q_n rate with respect to φ is derived as [73,74]

$$\frac{dQ_n}{d\varphi} = \frac{c_v}{R}\left(p\frac{dV}{d\varphi} + V\frac{dp}{d\varphi} - \frac{pV}{m}\frac{dm}{dt}\right) + p\frac{dV}{d\varphi} + h_e\frac{dm_e}{d\varphi} \tag{1}$$

where the gas equation of state

$$pV = mRT \tag{2}$$

In the equations above, h_e is the specific enthalpy of the cylinder content, while c_v and R are the specific heat capacity under constant volume and the specific gas constant, respectively. The instantaneous mass m in the cylinder at any crank angle φ (corresponding time t) is calculated from

$$m(\varphi) = m(\varphi_{IVC}) - \int_{\varphi_{IVC}}^{\varphi} \frac{dm_e}{dt}\frac{1}{6N_s}d\varphi \tag{3}$$

where a computation of mass is accomplished at the point of IVC (inlet valve closure), with known pressure and temperature there for the engine in hand According to Ref. [75], the T at IVC was selected 40 K higher than the after-cooler exhaust air temperature. Note that $d\varphi = 6N_s dt$, with N_s the engine speed in rpm.

Thus, the corresponding gross heat release Q_g rate with respect to φ, which is the energy released from the combustion of fuel, is given by

$$\frac{dQ_g}{d\varphi} = \frac{dQ_n}{d\varphi} + \frac{dQ_w}{d\varphi} \tag{4}$$

where the $dQ_w/d\varphi$ term stands for the rate of heat transferred to the walls of the combustion chamber; it is calculated by using the formula of Annand [76] that provides the dQ_w/dt heat loss rate term.

Obviously, by knowing the fuel lower calorific value Θ, the fuel burned mass rate with respect to φ in the chamber is computed from

$$\frac{dm_{fb}}{d\varphi} = \frac{1}{\Theta}\frac{dQ_g}{d\varphi} \tag{5}$$

The cylinder volume V and its rate of change with respect to crank angle $dV/d\varphi$ are calculated by standard expressions [2,77]. The blow-by rate dm_e/dt is calculated by using the well-known correlation for gas mass flow through a restriction accounting for one-dimensional, quasi-steady, compressible flow [1,73].

If now Eqs. (4) and (5) are integrated from the point of IVC event up to any crank angle φ of the closed part of the cycle (along the lines of Eq. (3)), one can obtain the respective cumulative values in the chamber of the heat released by the fuel Q_g and the fuel mass burned m_{fb}.

5.3. Combustion reaction and working medium properties

In this subsection only the combustion phase is addressed, since the compression and expansion phases can be considered as simple sub-cases (absence of chemical reaction and constant composition in time for compression). Although dissociation could be included [36,37], it was opted to neglect it for keeping the analysis simple. Moreover, in the light of the inherent uncertainties involved in experimental heat release analysis calculations, it was felt that its inclusion would not add much.

The basic stoichiometric chemical equation for the fuel used (with chemical formula $C_xH_yO_z$) – oxygen reaction is [73,77]

$$C_xH_yO_z + [x + (y/4) - (z/2)]O_2 \rightarrow xCO_2 + (y/2)H_2O \tag{6}$$

The number of kmoles b_i of the constituents (i = 1, 2, 3, 4 and 5 for CO_2, H_2O, O_2, N_2 and $C_xH_yO_z$, respectively) at any time t (or the corresponding crank angle φ), for complete combustion in air, are calculated from the following expressions:

$$b_1 = xw_f, b_2 = (y/2)w_f, b_3 = -b_1 - b_2/2 + w_f G/\Phi, b_4 = 3.76w_f G/\Phi, b_5 = w_{0f} - w_f \tag{7a}$$

where $G = x + (y/4) - (z/2)$, and $w_f = m_{fb}/M_f$ is the number of kmoles of fuel (with molecular weight M_f) burned up to that time out of a total of w_{0f}, with $b_5 = 0$ when $\Phi \leqslant 1$.

The fuel–air equivalence ratio Φ, i.e. the actual fuel–air ratio (by mass) divided by its stoichiometric value, is computed with the cumulative values (up to the crank angle in question) of the air and fuel burned (calculated in the previous subsection) as follows:

$$\Phi = [m_{fb}/(m - m_{fb})]/FA_{st} \tag{7b}$$

$$\text{with} \quad FA_{st} = (12x + y + 16z)/[4.76(x + y/4 - z/2)28.96] \tag{7c}$$

The specific internal energies (considering only their sensible part) of the components are given as 4th order polynomial expressions of the absolute temperature T [77]. Similar expressions are then derived for the specific enthalpies, specific heat capacities and specific heat capacities ratio, by applying the simple thermodynamic relations connecting these quantities for a perfect gas [73,74,77]. The mixture properties in the chamber are then computed by knowing the prevailing gas composition, as calculated from Eqs. (7a)–(7c), and the gas temperature T calculated from Eq. (2).

The equations of the thermodynamic model are solved numerically step-by-step using a simple time marching technique. The differential equations are converted to algebraic ones using a

simple Euler scheme. The associated computer program is written in Fortran V language and executed on a Pentium IV PC.

6. Presentation and discussion of combustion heat release analysis results

It is pointed out that only the results for the neat diesel fuel, the blend of 10% ethanol in the diesel fuel, and the blend of 16% *n*-butanol in the diesel fuel, denoted hereafter and in the figures as 'Et10-D' and 'Bu16-D', respectively, will be shown. This is dictated, on the one hand, for the sake of brevity of space of this paper and, on the other, by the differences in the respective diagrams that are relatively well discernible in this case. Results are given at the speed of 1200 rpm, for all the three loads considered of 20%, 40% and 60%, i.e. low, medium and high. It is to be noted that in all diagrams of this section, 'hot' TDC corresponds to 180° of crank angle φ. It is understood that all the pressure diagrams to be presented are 'mean-smooth' from the measured ones, as explained in the previous section, which are then processed to produce the other related parameters.

Fig. 2a shows for the speed of 1200 rpm, at the three loads considered, the fuel (injection) pressure against crank angle diagrams for the neat diesel fuel and the Et10-D blend. First it can be seen, as expected, that the injection duration increases with engine load for the two fuels and the same holds true for the injection pressures. It can be observed that for all loads considered, the fuel pressure diagrams for the Et10-D blend against the corresponding ones for the neat diesel fuel case do not show any appreciable differences in the injection duration or maximum pressure.

For the two lower loads the injection pulse has almost the same shape for the two fuels at each load, unlike the high load case where an 'hesitant hump' is observed after the first rise with the Et10-D blend. Note that in the case of high load, the residual fuel pressure in the connecting pipe is lower, a fact attributed to the particular functioning of the present injection pump system that is forced to have then a much delayed pump spill timing (static injection), for NO_x reduction, as mentioned in Section 2.

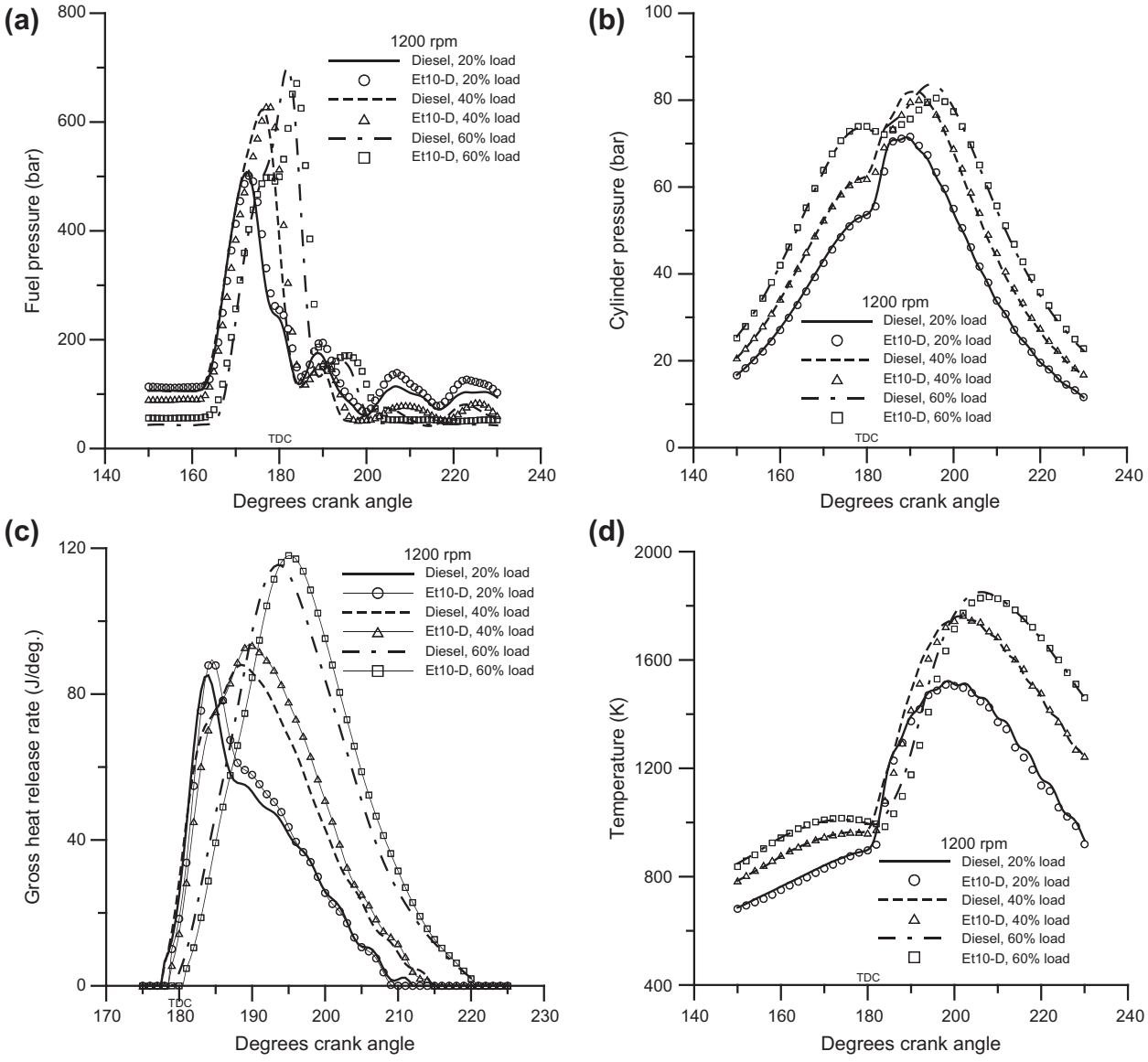

Fig. 2. Fuel (injection) pressure (a), cylinder pressure (b), gross heat release rate (c), and cylinder temperature (d), against crank angle diagrams for the neat diesel fuel and the 10% ethanol blend for the three loads at 1200 rpm.

The noticeable high displacement at the high load of the injection pulse is, of course, attributed to that deliberate delay of static injection timing.

All Et10-D blend diagrams show a very slight displacement-delay with respect to the corresponding ones with diesel fuel and so present delayed dynamic injection timings. This behavior is attributed to the different densities and bulk moduli of elasticity (cf. values in Table 2) influencing the whole injection process [38], while the static injection timing (at pump spill) was kept constant at each load. The latter behavior is explained qualitatively in detail in Refs. [33,38], where the simplified analysis of Obert [78] is followed. The latter can capture the idiosyncrasies of the high-pressure injection system and the effect of the different physical properties of the fuels used on the values of the fuel injection rate, injection pressures (with a rectangular profile) and dynamic injection timing.

Fig. 2b shows for the speed of 1200 rpm, at the three loads considered, the cylinder pressure against crank angle diagrams for the neat diesel fuel and the Et10-D blend, focusing on their part around TDC. First it can be seen, as expected, that the pressures increase with load, while the compression lines remain the same at each load and increase with load due to the turbocharger action. All Et10-D blend diagrams show slightly lower maximum pressures with respect to the corresponding ones with diesel fuel, a fact attributed to the delayed combustion with the Et10-D blend. The latter is attributed to the delayed dynamic injection timing mentioned above (in the discussion of Fig. 2a) and to the higher ignition delay of ethanol due to its lower cetane number (cf. values in Table 2).

Fig. 2c shows for the speed of 1200 rpm, at the three loads considered, the gross heat release rate against crank angle diagrams for the neat diesel fuel and the Et10-D blend, focusing on their part around TDC. First it can be seen, as expected, that the heat release rate values increase with engine load for both fuels. For the lower load, both parts of combustion, i.e. the premixed combustion (the part under the first 'abrupt peak') and the diffusion combustion (the last part under the second 'rounded peak') are apparent, but with the diffusion combustion possessing a minor role. For the

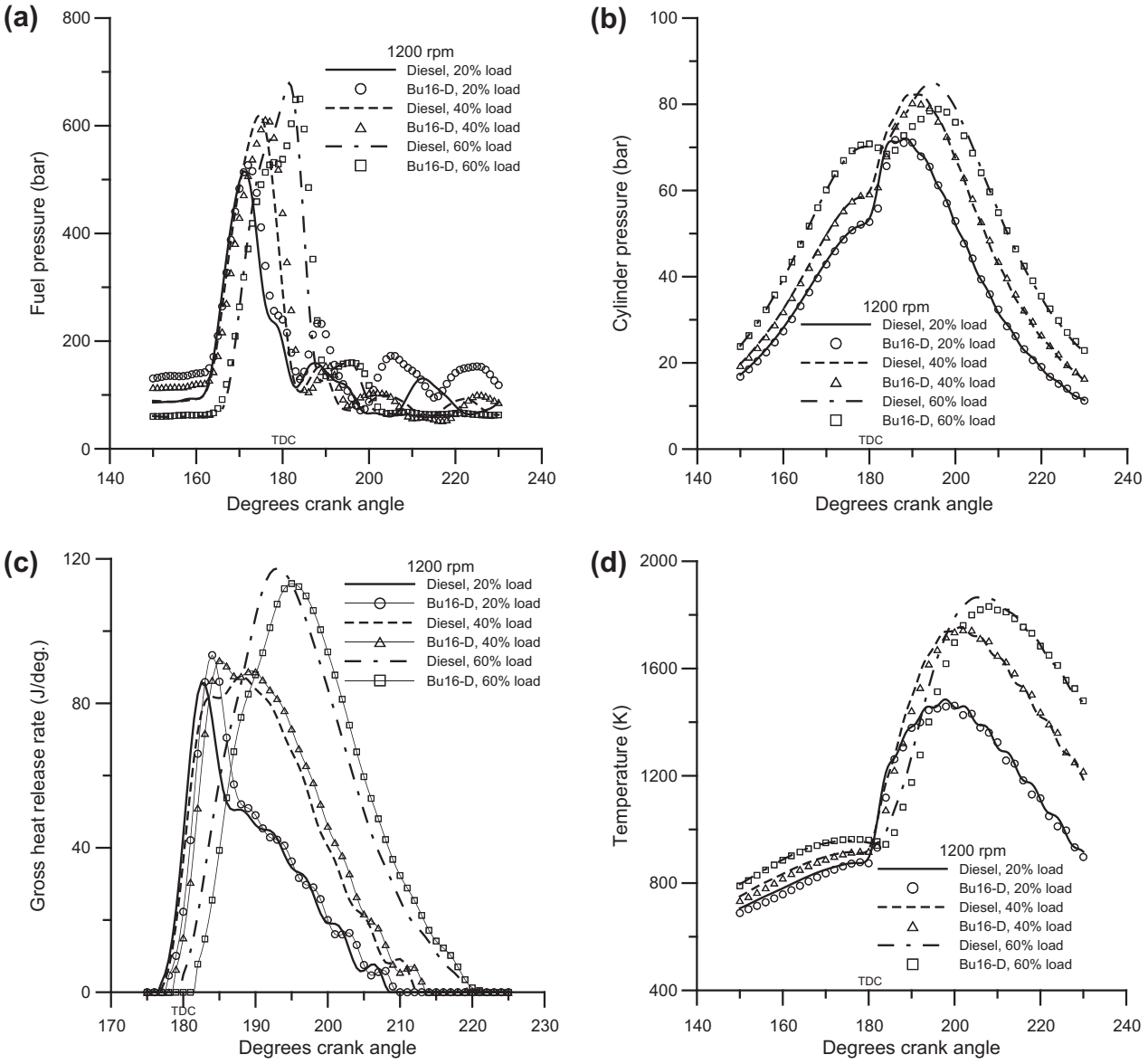

Fig. 3. Fuel (injection) pressure (a), cylinder pressure (b), gross heat release rate (c), and cylinder temperature (d), against crank angle diagrams for the neat diesel fuel and the 16% *n*-butanol blend for the three loads at 1200 rpm.

higher loads, the premixed combustion part tends to disappear with the diffusion combustion prevailing. For the 20% load considered the premixed combustion peak for the Et10-D is higher and sharper, and for the 40% not well discernible (for the corresponding case of 40% load for the *n*-butanol blend (see later Fig. 3c) it is better discernible). It is the lower cetane number of ethanol (cf. values in Table 2) that causes the increase of ignition delay and so the increased amount of 'prepared' fuel (to this end may also assist the easier evaporation of ethanol) for combustion after the start of ignition. However, as noticed in Fig. 2b, this is translated into slightly lower maximum pressures, probably because of the more than offsetting effect of later combustion in a lower temperature environment.

Fig. 2d shows for the speed of 1200 rpm, at the three loads considered, the cylinder temperature against crank angle diagrams for the neat diesel fuel and the Et10-D blend, focusing on their part around TDC. First it can be seen, as expected, that there is a temperature increase with engine load for both fuels. One can observe that for each load considered, the temperatures for the Et10-D blend are slightly displaced due to the delayed start of combustion mentioned above, being for the first part of combustion (~20–30° CA) lower than the corresponding ones for the neat diesel fuel case while leveling off later. It is stated, however, that this is a computed 'mixed' mean temperature due to the inherent single-zone modeling assumptions of the heat release analysis followed, so that these results must be interpreted with caution. Actually, as reported in [57], measured in-cylinder temperatures during the combustion stage showed much lower temperatures for the case of a 15% (by vol.) ethanol in diesel blend; the same is expected to hold true for *n*-butanol too, most likely at a lesser extent. The single-zone modeling assumption 'rounds' these results, although it manages to capture qualitatively correctly this mechanism.

Fig. 3a–d shows, for the speed of 1200 rpm, at the three loads considered, for the neat diesel fuel and the Bu16-D blend, the fuel (injection) pressure, the cylinder pressure, the gross heat release rate and the cylinder temperature against crank angle diagrams, respectively. They are similar in quality to their corresponding diagrams in Fig. 2a–d, for the Et10-D blend. Further, for the same

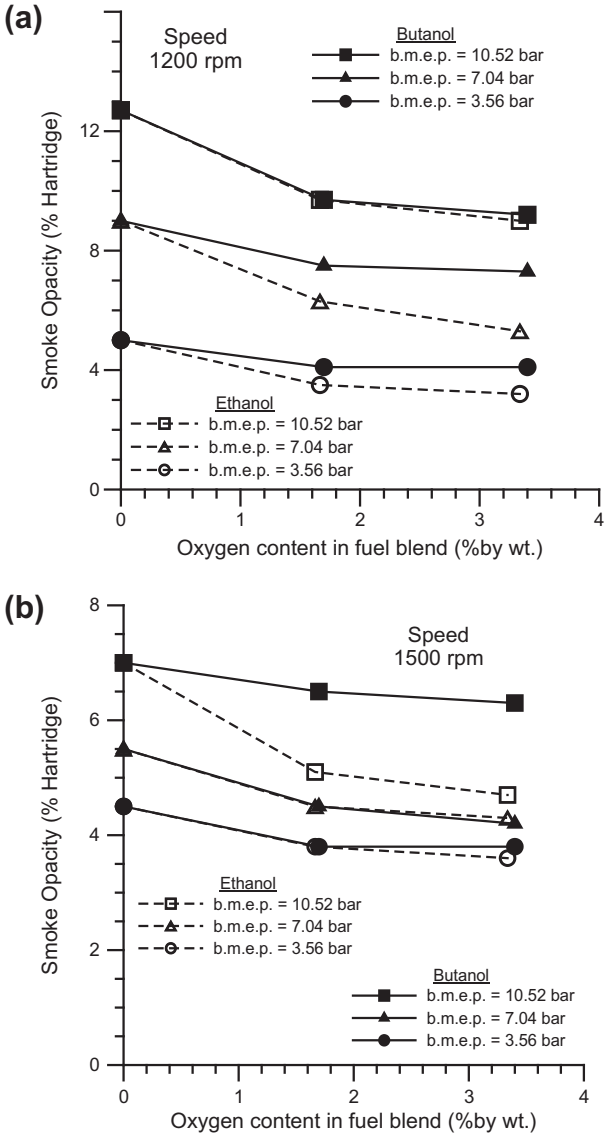

Fig. 4. Emitted (soot) smoke opacity (% Hartridge) for the neat diesel fuel, the 5% and the 10% ethanol blends, and the 8% and 16% *n*-butanol blends, for the three loads (b.m.e.p.), as a function of fuel-bound oxygen at 1200 rpm (a), and at 1500 rpm (b).

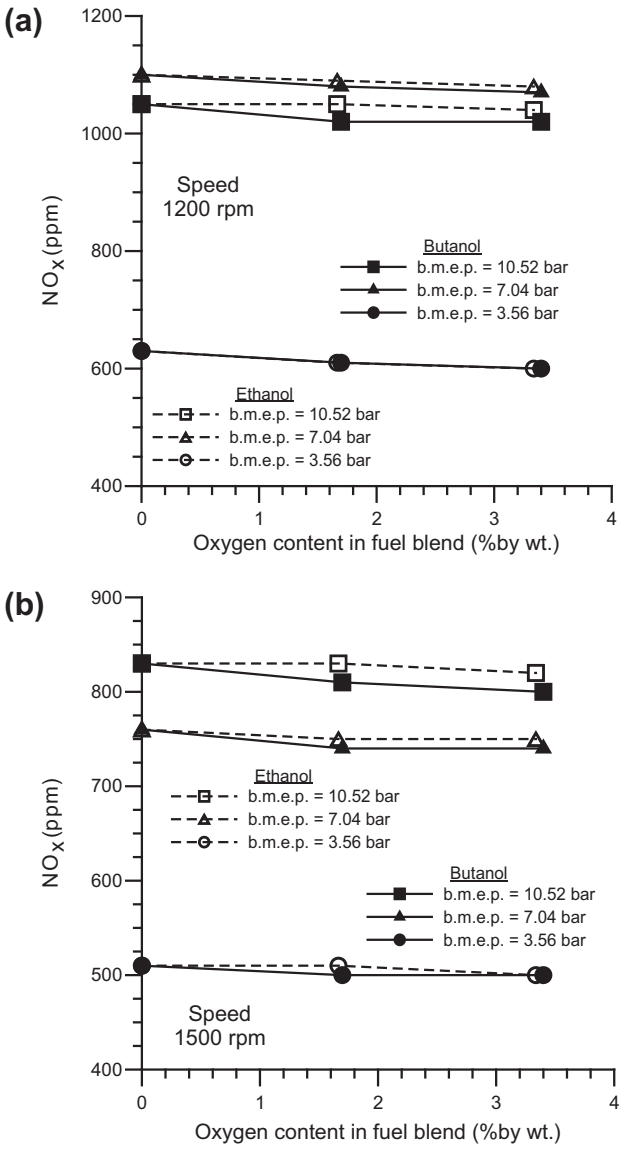

Fig. 5. Emitted nitrogen oxides (NO_x) in ppm for the neat diesel fuel, the 5% and the 10% ethanol blends, and the 8% and 16% *n*-butanol blends, for the three loads (b.m.e.p.), as a function of fuel-bound oxygen at 1200 rpm (a), and at 1500 rpm (b).

speed and load, the differences of the Et10-D blend and the Bu16-D blend from the corresponding neat diesel fuel case seem to be almost the same, inside the limits of the accuracy of the analysis.

This strengthens our belief that the choice of equal values of fuel-bound oxygen in the blends, for comparison of the combustion process, was a rational criterion at least in the way it is manifested in the single-zone (mixed mean) assumptions of an experimental heat release rate model. The present analysis is proved useful for interpreting the relative behavior between the blends of each bio-fuel against the neat diesel fuel case, unlike the case of comparison between the two bio-fuels concerning exhaust emissions and efficiency. This may require the specific details of the distribution of fuel–air ratio and temperatures inside the cylinder or even the influence of the specific structure of the fuels molecule, which falls outside the capabilities of the present model (and possibly of the state of the art) and the scope of this study.

Recourse is required to fundamental spray (physical parameters) and combustion (and chemical ones) studies using these bio-fuels. They seem to be extremely sparse, as in Refs. [79–81], so that more fundamental research work is called for on this area. The third very recent one [81] is notable, in the sense of dealing with fundamental flame studies of ethanol and butanol.

7. Discussion of the experimental performance and emissions results

It is stated that all figures to follow in this section, provide each emission or performance parameter for the neat diesel fuel and its blends with 5% and 10% ethanol or with 8% and 16% (by vol.) *n*-butanol, at the three loads considered (20%, 40% and 60% of the full load), for the engine speeds of 1200 and 1500 rpm. To effect comparison between ethanol and *n*-butanol blends, all diagrams have as independent (x) variable the fuel-bound oxygen in the blend, where one can see the almost equal values for this important variable, influencing strongly the combustion behavior and consequently the emissions formation (cf. discussion at the end of Section 3). Soot (smoke) and nitrogen oxides (NO_x) exhaust

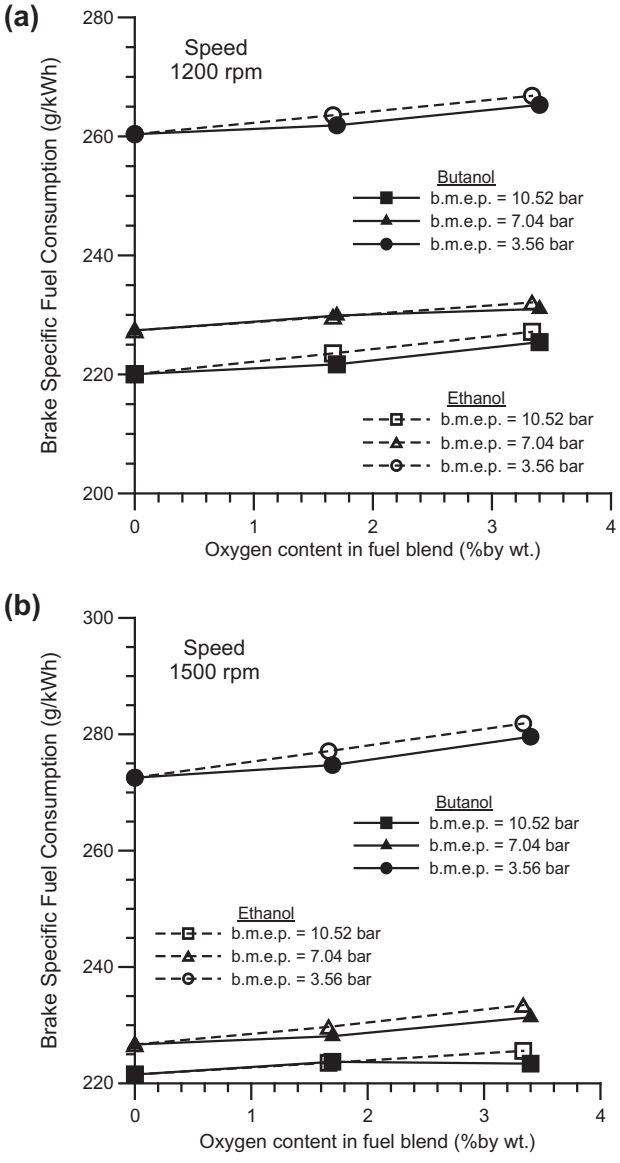

Fig. 6. Brake specific fuel consumption for the neat diesel fuel, the 5% and the 10% ethanol blends, and the 8% and 16% *n*-butanol blends, for the three loads (b.m.e.p.), as a function of fuel-bound oxygen at 1200 rpm (a), and at 1500 rpm (b).

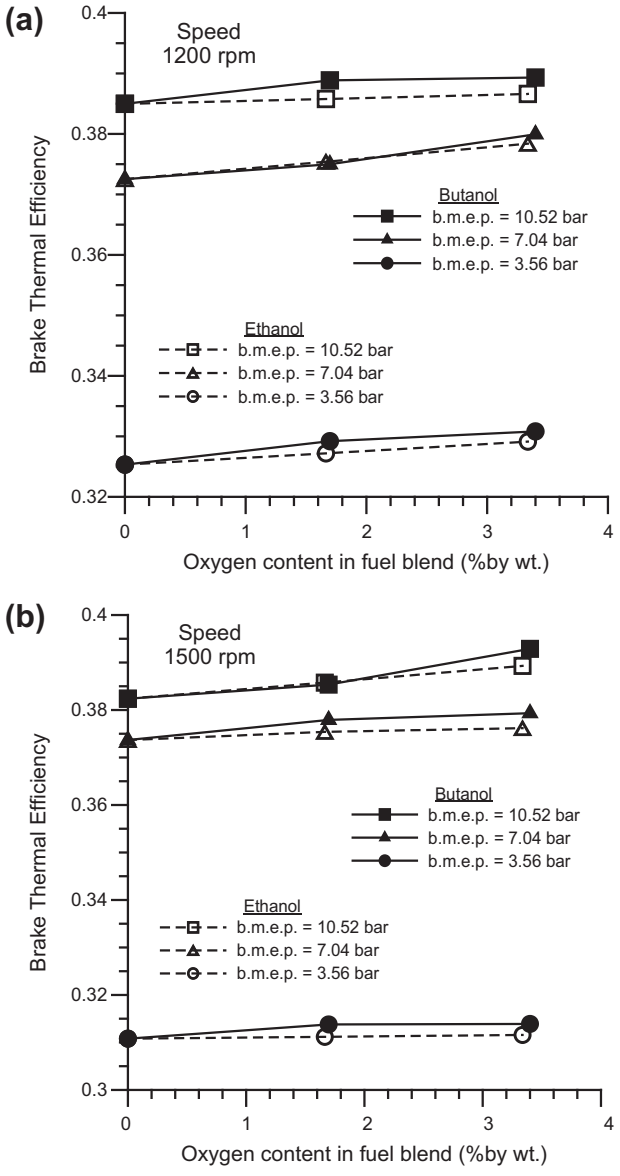

Fig. 7. Brake thermal efficiency for the neat diesel fuel, the 5% and the 10% ethanol blends, and the 8% and 16% *n*-butanol blends, for the three loads (b.m.e.p.), as a function of fuel-bound oxygen at 1200 rpm (a), and at 1500 rpm (b).

emissions that are of high importance for diesel engines, and specific fuel consumption and brake thermal efficiency measurements results will be treated here.

The fundamental studies concerning physical (e.g. spray behavior) or chemical aspects of *n*-butanol at engine conditions are absent, while the ethanol ones are very sparse. Therefore, in order to aid the correct interpretation of the observed engine behavior, the combustion heat release analysis results presented in the previous section will be used, taking also into account the differing physical and chemical properties of ethanol and *n*-butanol against those for the diesel fuel.

Fig. 4a and b shows the emitted (soot) smoke opacity (% Hartridge) for the neat diesel fuel, the 5% and the 10% ethanol blends, and the 8% and 16% *n*-butanol blends, for the three loads (b.m.e.p.), as a function of fuel-bound oxygen in the blend, at engine speeds of 1200 rpm and 1500 rpm, respectively. One can see that the soot emitted by the ethanol/diesel fuel or *n*-butanol/diesel fuel blends is significantly lower than that for the corresponding neat diesel fuel case, with the reduction being higher the higher the percentage of either bio-fuel in the blend, i.e. with increasing fuel-bound oxygen content. This is attributed to the combustion being now assisted by the presence of the fuel-bound oxygen of either bio-fuel even in locally rich 'zones', which seems to have the dominant influence [6,7]. It was reported in Refs. [57,58] that in-cylinder combustion photography showed indeed lower luminosity flames for the corresponding ethanol blends, revealing the lower net soot produced, and this is expected to be applicable for *n*-butanol too. For the explanation of the relative superiority observed in some cases of the ethanol blends over the *n*-butanol ones, in reducing more the emitted soot, it may be argued that this is due to locally higher temperatures contributing to its higher oxidation rates inside the crucial 'zones', and/or to the structure of the fuels molecule (cf. discussion at the end of the previous section).

Fig. 5a and b shows the nitrogen oxides (NO_x) exhaust emissions (in ppm) for the neat diesel fuel, the 5% and the 10% ethanol blends, and the 8% and 16% *n*-butanol blends, for the three loads (b.m.e.p.), as a function of fuel-bound oxygen in the blend, at engine speeds of 1200 rpm and 1500 rpm, respectively. Firstly, it can be observed that at the speed of 1200 rpm NO_x at 40% load is higher than that of 60% load, while at 1500 rpm this behavior is inverted. The explanation is that at the lower speed the decrease of the injection timing at the higher load (as stated in Section 2, the static injection timing of the engine is reduced at high loads for the purpose of reducing nitrogen oxides emissions to meet the Euro II emission standards) curbs the value of NO_x, unlike the case of the higher speed case where it seems that the increased temperatures more than offset it.

Further, one can see in those figures that the NO_x emitted by the ethanol/diesel fuel or *n*-butanol/diesel fuel blends is equal or slightly lower than that for the corresponding neat diesel fuel case, with the reduction being higher the higher the percentage of either bio-fuel in the blend, i.e. with increasing fuel-bound oxygen content. This is attributed to the little lower temperatures during the first part of combustion having the dominant influence, when nitric oxide (NO) formation is imminent, with the influence of 'local' oxygen playing a secondary role. The explanation of the relative slight inferiority observed in some cases of the ethanol blends over the *n*-butanol ones, in reducing less the emitted NO_x, requires recourse to more fundamental spray and combustion studies using these bio-fuels, which are not available (cf. discussion at the end of the previous section).

Fig. 6a and b shows the brake specific fuel consumption (b.s.f.c., in g/kWh) for the neat diesel fuel, the 5% and the 10% ethanol blends, and the 8% and 16% *n*-butanol blends, for the three loads (b.m.e.p.), as a function of fuel-bound oxygen in the blend, at engine speeds of 1200 rpm and 1500 rpm, respectively. Since the comparison is effected at the same load (b.m.e.p.) and speed, which is translated into the same engine brake power [73,74], the b.s.f.c. values are then effectively directly proportional to the fuel mass flow rate values. It is observed that for all the bio-fuels blends, the b.s.f.c. is a little higher than the corresponding diesel fuel case, with the increase being higher the percentage of bio-fuels in the blend. This is the expected behavior due to the lower calorific value of the bio-fuels compared to that for the neat diesel fuel (cf. values in Table 2), thus requiring higher fuel mass flow rates in order to achieve the same load. The relatively increased b.s.f.c. values of the ethanol/diesel fuel over the *n*-butanol/diesel fuel blends, at the same operating conditions, is explained by the same logic, i.e. that the lower calorific value of ethanol is lower than that of the *n*-butanol one.

Fig. 7a and b shows the brake thermal efficiency (b.t.e.) for the neat diesel fuel, the 5% and the 10% ethanol blends, and the 8% and 16% *n*-butanol blends, for the three loads (b.m.e.p.), as a function of fuel-bound oxygen in the blend, at engine speeds of 1200 rpm and 1500 rpm, respectively. It is observed that for all the bio-fuels blends, the b.t.e. is very slightly higher than that for the corresponding neat diesel fuel case, with the increase being higher the higher the percentage of the bio-fuels in the blend. This means that the increase of b.s.f.c. for the bio-fuel blends is lower than the corresponding decrease of the lower calorific value of the blends, by noting that the brake thermal efficiency is simply the inverse of the product of the specific fuel consumption and the lower calorific value of the fuel [73,74]. Since the differences are very small, one is very hesitant to provide (speculative) explanations for the results of the present analysis that refers to a phenomenon that depends on so many factors (spray details, fuel properties, etc.), usually with counteracting influence.

8. Conclusions

An extended experimental study is conducted to evaluate the effects of using blends of diesel fuel with either ethanol in proportions of 5% and 10% or *n*-butanol in 8% and 16% (by vol.), on the combustion behavior of a fully-instrumented, six-cylinder, turbocharged and after-cooled, heavy duty (HD), direct injection (DI), 'Mercedes-Benz' engine installed at the authors' laboratory.

The series of tests are conducted using each of the above bio-fuels blends, with the engine working at three loads and at engine speeds of 1200 and 1500 rpm. In each test, exhaust regulated emissions are measured as well as brake specific fuel consumption and thermal efficiency.

Fuel injection and cylinder pressure diagrams were obtained for each test case. A heat release analysis of the experimentally obtained combustion chamber pressure diagrams is developed and used, with the pertinent application of the energy and state equations. From the analysis results, plots of the history in the combustion chamber of the gross heat release rate and temperatures reveal some interesting features, which shed light into the combustion mechanism when using these bio-fuels blends, considering also the widely differing physical and chemical properties of these bio-fuels against those for the diesel fuel.

It is revealed that with the use of these bio-fuels blends against the neat diesel fuel case, the following hold:

- Fuel injection pressure diagrams are very slightly displaced (delayed).
- The ignition delay is increased.
- Maximum cylinder pressures are slightly reduced.
- Cylinder temperatures are reduced during the first part of combustion, leveling off later.

The heat release analysis results are used to aid the correct interpretation of the observed engine behavior emissions-wise, when using these bio-fuels blends against the neat diesel fuel case, that is:

- Reduction of smoke opacity with these blends.
- Reduction of smoke opacity with increasing percentage of bio-fuels in the blend.
- Reduction of nitrogen oxides with these blends.
- Reduction of nitrogen oxides with increasing percentage of bio-fuels in the blend.

References

[1] Rakopoulos CD, Giakoumis EG. Diesel engine transient operation – principles of operation and simulation analysis. London: Springer; 2009.
[2] Pulkrabek WW. Engineering fundamentals of internal combustion engines. 2nd ed. New Jersey: Pearson Prentice-Hall; 2004.
[3] Levendis YA, Pavlotos I, Abrams RF. Control of diesel soot, hydrocarbon and NO_x emissions with a particulate trap and EGR. SAE paper no. 940460; 1994.
[4] Larsen C, Oey F, Levendis YA. An optimization study on the control of NO_x and particulate emissions from diesel engines. SAE paper no. 960473; 1996.
[5] Komninos NP, Rakopoulos CD. Numerical investigation into the formation of CO and oxygenated and nonoxygenated hydrocarbon emissions from isooctane- and ethanol-fueled HCCI engines. Energy Fuels 2010;24:1655–67.
[6] Miyamoto N, Ogawa H, Nabi MN. Approaches to extremely low emissions and efficient diesel combustion with oxygenated fuels. Int J Engine Res 2000;1:71–85.
[7] Choi CY, Reitz RD. An experimental study on the effects of oxygenated fuel blends and multiple injection strategies on DI diesel engine emissions. Fuel 1999;78:1303–17.
[8] Rakopoulos CD, Michos CN, Giakoumis EG. Studying the effects of hydrogen addition on the second-law balance of a biogas-fuelled spark ignition engine by use of a quasi-dimensional multi-zone combustion model. Proc Inst Mech Eng, Part D, J Autom Eng 2008;222:2249–68.
[9] Abu-Jrai A, Rodriguez-Fernandez J, Tsolakis A, Megaritis A, Theinnoi K, Cracknell RF, et al. Performance, combustion and emissions of a diesel engine operated with reformed EGR. Comparison of diesel and GTL fuelling. Fuel 2009;88:1031–41.
[10] Hansen AC, Kyritsis DC, Lee CF. Characteristics of biofuels and renewable fuel standards. In: Vertes AA, Blaschek HP, Yukawa H, Qureshi N, editors. Biomass to biofuels – strategies for global industries. New York: John Wiley; 2009.
[11] Rickeard DJ, Thompson ND. A review of the potential for bio-fuels as transportation fuels. SAE paper no. 932778; 1993.
[12] Hansen AC, Zhang Q, Lyne PWL. Ethanol–diesel fuel blends – a review. Bioresour Technol 2005;96:277–85.
[13] Rakopoulos CD, Antonopoulos KA, Rakopoulos DC, Hountalas DT, Giakoumis EG. Comparative performance and emissions study of a direct injection diesel engine using blends of diesel fuel with vegetable oils or bio-diesels of various origins. Energy Convers Manage 2006;47:3272–87.
[14] Miers SA, Carlson RW, McConnell SS, Ng HK, Wallner T, Esper JL. Drive cycle analysis of butanol/diesel blends in a light-duty vehicle. SAE paper no. 2008-01-2381; 2008.
[15] Yao Mingfa, Wang Hu, Zheng Zunqing, Yue Yan. Experimental study of *n*-butanol additive and multi-injection on HD diesel engine performance and emissions. Fuel 2010;89:2191–201.
[16] Rakopoulos DC, Rakopoulos CD, Hountalas DT, Kakaras EC, Giakoumis EG, Papagiannakis RG. Investigation of the performance and emissions of a bus engine operating on butanol/diesel fuel blends. Fuel 2010;89:2781–90.
[17] Rakopoulos DC, Rakopoulos CD, Giakoumis EG, Dimaratos AM, Kyritsis DC. Effects of butanol-diesel fuel blends on the performance and emissions of a high-speed DI diesel engine. Energy Convers Manage 2010;51:1989–97.
[18] Graboski MS, McCormick RL. Combustion of fat and vegetable oil derived fuels in Diesel engines. Prog Energy Combust Sci 1998;24:125–64.
[19] Demirbas A. Biodiesel fuels from vegetable oils via catalytic and non-catalytic supercritical alcohol transesterifications and other methods: a survey. Energy Convers Manage 2003;44:2093–109.
[20] Baranescu RA, Lusco JJ. Sunflower oil as a fuel extender in direct injection turbocharged diesel engines. SAE paper no. 820260; 1982.
[21] Rakopoulos CD. Comparative performance and emission studies when using olive oil as a fuel supplement in DI and IDI Diesel engines. Renew Energy 1992;2:327–31.
[22] Rakopoulos CD, Rakopoulos DC, Hountalas DT, Giakoumis EG, Andritsakis EC. Performance and emissions of bus engine using blends of diesel fuel with bio-diesel of sunflower or cottonseed oils derived from Greek feedstock. Fuel 2008;87:147–58.
[23] Rakopoulos CD, Antonopoulos KA, Rakopoulos DC, Kakaras EC, Pariotis EG. Characteristics of the performance and emissions of a HSDI diesel engine running with cottonseed oil or its methyl ester and their blends with diesel fuel. Int J Vehicle Des 2007;45:200–21.
[24] Lapuerta M, Armas O, Ballesteros R, Fernandez J. Diesel emissions from biofuels derived from Spanish potential vegetable oils. Fuel 2005;84:773–80.
[25] Tsolakis A, Megaritis A, Wyszynski ML, Theinnoi K. Engine performance and emissions of a diesel engine operating on diesel-RME (rapeseed methyl ester) blends with EGR (exhaust gas recirculation). Energy 2007;32:2072–80.
[26] Bueno AV, Velasquez JA, Milanez LF. Effect of soybean oil ethyl ester/diesel fuel blends on engine efficiency. Int J Vehicle Des 2009;50:229–47.
[27] Bueno AV, Velasquez JA, Milanez LF. Heat release and engine performance effects of soybean oil ethyl ester blending into diesel fuel. In: Proc of the 22nd int conf 'ECOS 2009', Foz do Iguacu/Parana, Brazil; August 31–September 3, 2009. p. 2009–18.
[28] Papayannakos N, Rakopoulos CD, Kyritsis S, Lappas A, Chatzigakis A, Chlivinos G, et al. Pilot production and testing of bio-diesel produced from Greek feedstocks. In: Frangopoulos C, Rakopoulos C, Tsatsaronis G, editors. Proc of the 19th int conf 'ECOS 2006', vol. 3. Crete, Greece; July 12–14, 2006. p. 1489–97.
[29] Rakopoulos DC, Rakopoulos CD, Kakaras EC, Giakoumis EG. Effects of ethanol–diesel fuel blends on the performance and exhaust emissions of heavy duty DI diesel engine. Energy Convers Manage 2008;49:3155–62.
[30] Rakopoulos CD, Antonopoulos KA, Rakopoulos DC, Hountalas DT, Andritsakis EC. Study of the performance and emissions of a high-speed direct injection diesel engine operating on ethanol–diesel fuel blends. Int J Alternative Propul 2007;1:309–24.
[31] Rakopoulos CD, Antonopoulos KA, Rakopoulos DC. Experimental heat release analysis and emissions of a HSDI diesel engine fueled with ethanol–diesel fuel blends. Energy 2007;32:1791–808.
[32] Rakopoulos DC, Rakopoulos CD, Giakoumis EG, Papagiannakis RG, Kyritsis DC. Experimental-stochastic investigation of the combustion cyclic variability in HSDI diesel engine using ethanol–diesel fuel blends. Fuel 2008;87:1478–91.
[33] Rakopoulos CD, Rakopoulos DC, Giakoumis EG, Dimaratos AM. Investigation of the combustion of neat cottonseed oil or its neat bio-diesel in a HSDI diesel engine by experimental heat release and statistical analyses. Fuel 2010;89:3814–26.
[34] Rakopoulos CD, Rakopoulos DC, Giakoumis EG, Kyritsis DC. The combustion of *n*-butanol/diesel fuel blends and its cyclic variability in a DI diesel engine. Proc Inst Mech Eng, Part A, J Power Energy, in press.
[35] Rakopoulos CD, Giakoumis EG. Second-law analyses applied to internal combustion engines operation. Prog Energy Combust Sci 2006;32:2–47.
[36] Rakopoulos CD, Antonopoulos KA, Rakopoulos DC, Hountalas DT. Multi-zone modeling of combustion and emissions formation in DI diesel engine operating on ethanol–diesel fuel blends. Energy Convers Manage 2008;49:625–43.
[37] Rakopoulos CD, Antonopoulos KA, Rakopoulos DC. Development and application of a multi-zone model for combustion and pollutants formation in a direct injection diesel engine running with vegetable oil or its bio-diesel. Energy Convers Manage 2007;48:1881–901.
[38] Rakopoulos CD, Antonopoulos KA, Rakopoulos DC. Multi-zone modeling of diesel engine fuel spray development with vegetable oil, bio-diesel or diesel fuels. Energy Convers Manage 2006;47:1550–73.
[39] Kouremenos DA, Rakopoulos CD, Kotsos KG. A stochastic-experimental investigation of the cyclic pressure variation in a DI single-cylinder diesel engine. Int J Energy Res 1992;16:865–77.
[40] Sczomak DP, Henein NA. Cycle-to-cycle variation with low ignition quality fuels in a CFR diesel engine. Trans SAE 1979; 88:3124–44 [SAE paper no. 790924].
[41] Huang Z, Lu H, Jiang D, Zeng K, Liu B, Zhang J, et al. Combustion behaviors of a compression-ignition engine fuelled with diesel/methanol blends under various fuel delivery advance angles. Bioresource Technol 2004;95:331–41.
[42] Sayin C, Ilhan M, Canakci M, Gumus M. Effect of injection timing on the exhaust emissions of a diesel engine using diesel–methanol blends. Renew Energy 2009;34:1261–9.
[43] Likos B, Callahan TJ, Moses CA. Performance and emissions of ethanol and ethanol–diesel blends in direct-injected and pre-chamber diesel engines. SAE paper no. 821039; 1982.
[44] Ecklund EE, Bechtold RL, Timbario TJ, McCallum PW. State-of-the-art report on the use of alcohols in diesel engines. SAE paper no. 840118; 1984.
[45] Corkwell KC, Jackson MM, Daly DT. Review of exhaust emissions of compression ignition engines operating on E diesel fuel blends. SAE paper no. 2003-01-3283; 2003.
[46] Wrage KW, Goering CE. Technical feasibility of diesohol. Trans ASAE 1980;23(6):1338–43.
[47] Meiring P, Hansen AC, Vosloo AP, Lyne PWL. High concentration ethanol–diesel blends for compression-ignition engines. SAE paper no. 831360; 1983.
[48] Li D, Zhen H, Xingcai L, Wugao Z, Jianguang Y. Physico-chemical properties of ethanol–diesel blend fuel and its effect on performance and emissions of diesel engines. Renew Energy 2005;30:67–76.
[49] Schaefer AJ, Hardenberg HO. Ignition improvers for ethanol fuels. SAE paper no. 810249; 1981.
[50] Simonsen H, Chomiak J. Testing and evaluation of ignition improvers for ethanol in a DI diesel engine. SAE paper no. 952512; 1995.
[51] Satge de Caro P, Mouloungui Z, Vaitilingom G, Berge JCh. Interest of combining an additive with diesel–ethanol blends for use in diesel engines. Fuel 2001;80:565–74.
[52] Shropshire GJ, Goering CE. Ethanol injection into a diesel engine. Trans ASAE 1982;25(3):570–5.

[53] Hayes TK, Savage LD, White RA, Sorenson SC. The effect of fumigation of different ethanol proofs on a turbocharged diesel engine. SAE paper no. 880497; 1988.
[54] Noguchi N, Terao H, Sakata C. Performance improvement by control of flow rates and diesel injection timing on dual-fuel engine with ethanol. Bioresour Technol 1996;56:35–9.
[55] Boruff PA, Schwab AW, Goering CE, Pryde EH. Evaluation of diesel fuel–ethanol microemulsions. Trans ASAE 1982;25(1):47–53.
[56] Ajav EA, Singh B, Bhattacharya TK. Experimental study of some performance parameters of a constant speed stationary diesel engine using ethanol–diesel blends as fuel. Biomass Bioenergy 1999;17:357–65.
[57] Xingcai L, Zhen H, Wugao Z, Degang L. The influence of ethanol additives on the performance and combustion characteristics of diesel engines. Combust Sci Technol 2004;176:1309–29.
[58] Chen H, Shuai S, Wang J. Study on combustion characteristics and PM emission of diesel engines using ester–ethanol–diesel blended fuels. Proc Combust Inst 2007;31:2981–9.
[59] Eseji T, Qureshi N, Blaschek HP. Production of acetone–butanol–ethanol (ABE) in a continuous flow bioreactor using degermed corn and clostridium beijernickii. Process Biochem 2007;42:34–9.
[60] Chotwichien A, Luengnaruemitchai A, Jai-In S. Utilization of palm oil alkyl esters as an additive in ethanol–diesel and butanol–diesel blends. Fuel 2009;88:1618–24.
[61] Johnson DT, Taconi KA. The glycerin glut: options for the value-added conversion of crude glycerol resulting from biodiesel production. AIChE, Environ Prog Sustain Energy 2007;26:338–48.
[62] Taconi KA, Venkataramanan KP, Johnson DT. Growth and solvent production by clostridium pasteurianum (ATCC, 6013) utilizing biodiesel-derived crude glycerol as the sole carbon source. AIChE, Environ Prog Sustain Energy 2009;28:100–10.
[63] Pucher H, Sperling E. *n*-Butanol–Diesel-Gemisch als Alternativekraftstoff fuer den Dieselmotor. Erdoel und Kohle, Erdgas, Petrochemie vereinigt mit Brennstoff-Chemie 1986;39:353–6 (in German).
[64] Yoshimoto Y, Onodera M, Tamaki H. Performance and emission characteristics of diesel engines fueled by vegetable oils. SAE paper no. 2001-01-1807/4227; 2001.
[65] Yoshimoto Y, Onodera M. Performance of a diesel engine fueled by rapeseed oil blended with oxygenated organic compounds. SAE paper no. 2002-01-2854; 2002.
[66] Huang J, Wang Y, Li S, Roskilly AP, Yu H, Li H. Experimental investigation on the performance and emissions of a diesel engine fuelled with ethanol–diesel blends. Appl Therm Eng 2009;29:2484–90.
[67] Rakopoulos CD, Dimaratos AM, Giakoumis EG, Rakopoulos DC. Investigating the emissions during acceleration of a turbocharged diesel engine operating with bio-diesel or *n* -butanol diesel fuel blends. Energy 2010;35:5173–84.
[68] Theobald MA, Alkidas AC. On the heat-release analysis of diesel engines: effects of filtering of pressure data. SAE paper no. 872059; 1987.
[69] Homsy SC, Atreya, A. An experimental heat release rate analysis of a diesel engine operating under steady state conditions. SAE paper no. 970889; 1997.
[70] Rakopoulos CD, Antonopoulos KA, Rakopoulos DC, Giakoumis EG. Study of combustion in a divided chamber turbocharged diesel engine by experimental heat release analysis in its chambers. Appl Therm Eng 2006;26:1611–20.
[71] Payri F, Lujan JM, Martín J, Abbad A. Digital signal processing of in-cylinder pressure for combustion diagnosis of internal combustion engines. Mech Syst Signal Process 2010;24:1767–84.
[72] Bueno AV, Velasquez JA, Milanez LF. A new engine indicating measurement procedure for combustion heat release analysis. Appl Therm Eng 2009;29:1657–75.
[73] Heywood JB. Internal combustion engine fundamentals. New York: McGraw-Hill; 1988.
[74] Ferguson CR. Internal combustion engines. New York: Wiley; 1986.
[75] Zinner K. Supercharging of internal combustion engines. Berlin: Springer; 1978.
[76] Annand WJD. Heat transfer in the cylinders of reciprocating internal combustion engines. Proc Inst Mech Engrs 1963;177:973–90.
[77] Benson RS, Whitehouse ND. Internal combustion engines. Oxford: Pergamon; 1979.
[78] Obert EF. Internal combustion engines and air pollution. New York: Intext Educ. Publ; 1973.
[79] Pepiot-Desjardins P, Pitsch H, Malhotra R, Kirby SR, Boehman AL. Structural group analysis for soot reduction tendency of oxygenated fuels. Combust Flame 2008;154:191–205.
[80] Zhang Yu, Boehman AL. Oxidation of 1-butanol and a mixture of *n*-heptane/1-butanol in a motored engine. Combust Flame 2010;157:1816–24.
[81] Agathou MS, Kyritsis DC. An experimental comparison of non-premixed bio-butanol flames with the corresponding flames of ethanol and methane. Fuel 2011;90:255–62.